Source identification and risk analysis of potentially toxic elements (PTEs) in rainwater runoff from a manganese mine (south central Hunan, China)

Xin Luo, Bozhi Ren, Andrew S. Hursthouse, Feng Jiang, Ren-jian Deng and Zhenghua Wang

ABSTRACT

Potentially toxic elements (PTEs) in manganese ore areas are prevalent in rainwater runoff and pose a major threat to human health. In this study, field investigation and geostatistical analysis methods of positive matrix factorization (PMF) and geographic information systems (GIS) were used to systematically study the pollution in rainwater runoff from a manganese mining area in Xiangtan, China, to evaluate source contributions for the health risk assessment of PTEs. The average concentrations (mg/L) of six PTEs were: 0.3357 (Mn), 0.0450 (Ni), 0.0106 (Cu), 0.0148 (Zn), 0.0068 (Cd) and 0.0390 (Pb). The coefficients of variation (CV) for Mn and Zn were >180% and >130%, with the other analytes having values below 70%. The GIS and PMF analysis produced more refined spatial source apportionments, including mining, smelting, transportation, agricultural production and natural sources. The results of the health risk assessment showed that the non-carcinogenic risk was negligible, and the carcinogenic risk was potentially dangerous but acceptable for both adults and children. In addition, the children's total carcinogenic risk value was greater than that of adults, highlighting their vulnerability. This study demonstrates the potential of PMF to provide a framework to spatially prioritize treatment objectives within the mining region to improve environmental conditions.

Key words | health risk assessment, positive matrix factorization (PMF), potentially toxic elements, rainwater runoff, source analysis

Xin Luo
Bozhi Ren (corresponding author)
Andrew S. Hursthouse
Feng Jiang
Ren-jian Deng
Zhenghua Wang
Hunan Provincial Key Laboratory of Shale Gas Resource Exploitation,
Xiangtan 411201,
China
E-mail: *bozhiren@126.com*

Xin Luo
Bozhi Ren
Feng Jiang
Ren-jian Deng
Zhenghua Wang
School of Civil Engineering,
Hunan University of Science and Technology,
Xiangtan 411201,
China

Andrew S. Hursthouse
School of Computing Engineering & Physical Sciences,
University of the West of Scotland,
Paisley PA1 2BE,
UK

HIGHLIGHTS

- Mn is the most serious contaminating element in rainwater runoff.
- PMF was used to analyze five sources of PTEs in rainwater runoff.
- These present no health risks in the region.

INTRODUCTION

A number of potentially toxic elements (PTEs) have been highlighted as priority contaminants globally and have received widespread attention due to their persistence and toxicity to humans and organisms (Liu *et al.* 2017). Prolonged exposure to an environment containing PTEs can cause a wide range of diseases; for example, excessive manganese (Mn) in the human body may lead to mental illness, as well as more serious Parkinson's disease (Li *et al.* 2018). High environmental levels of lead (Pb) can lead to high blood Pb (Pareja-Carrera *et al.* 2014). In areas of localized mineral exploitation, continuous mining activities, industrial processing, more widespread subsistence agriculture activities and

doi: 10.2166/ws.2020.352

transportation, there are numerous sources and pathways for wider environmental contamination and the exposure of workers and residents. This is particularly evident in the manganese mining area of Xiangtan, south central China, where prolonged exploitation activities have led to the movement of manganese and other PTEs into the soil by a number of routes, resulting in excessive soil pollution (Cao *et al.* 2017; Ren *et al.* 2017; Li *et al.* 2018). Under the action of rainfall, especially in subtropical climate zones, rainwater runoff provides a potentially significant pathway for a wider pollution impact on the local environment and can lead to significant exposure and potential harm to human health (Yang *et al.* 2011; Tang *et al.* 2017). Addressing these key issues is an urgent priority, since resolving a wide range of localized cases will support the future phase of national economic and social development.

A number of quantitative statistical models, such as chemical mass balance (CMB), principal component analysis (PCA) and positive matrix factorization (PMF), have previously been used in pollution source analysis (Soonthornnonda & Christensen 2008; Huang *et al.* 2016). Among them, PMF has only recently been applied to identify sources of PTEs (Huang *et al.* 2018; Xiao *et al.* 2019b). In addition, the spatial power of geographic information systems (GIS) and statistical analysis (using SPSS) allow data outliers to be accurately distinguished. In combination with this, identifying the hot spot locations of high PTE concentrations at a specific location can aid in the reduction of uncertainty and the cost of assessment. This approach has been used to determine spatial structure characteristics and pollution levels and perform source analysis in a number of cases, including assessment of surface sediments, soil organic matter variation, the distribution of sulfur species in paddy soils, pollutant metal and microbial community responses in soil, quality of water in gulf zones and metals in mine soil (Herbert *et al.* 2014; Bellanco & Sánchez-Leal 2016; Cao *et al.* 2017; Yang *et al.* 2017; Yang *et al.* 2018). However, there are few examples of studies on rainwater runoff from mining sites, which is therefore an overlooked topic in many locations. In this study, we describe a detailed investigation of PTE content in rainwater runoff from a large-scale manganese mining site using a combination of PMF and GIS mapping.

Xiangtan is an old industrial base in Hunan Province (China) which possesses rich mineral resources, including manganese. Since 1913, large quantities of manganese ores have been exploited, and long-term mining, tailings production and smelting activities have led to very serious environment degradation. Ren *et al.* (2015) previously determined the average concentrations of six PTEs: Mn, nickel (Ni), copper (Cu), zinc (Zn), cadmium (Cd) and Pb in rainwater runoff in the region, and attempted source identification using PCA. That study lacked true spatial resolution, highlighting varied enrichment between PTEs and limited source identification to three factors.

The objectives of the research described in this study are to: (1) build a spatially refined hot spot map of pollution in surface waters in the region; (2) apply an analysis using PMF to evaluate potential sources of six PTEs; (3) extrapolate environmental conditions to assess the health risks of six PTEs to local residents. This study intends to improve the use of site-specific information to understand the extent of impacts and provide an improved framework to manage, prevent and control further pollution, thus providing a scientific basis for health risk assessment in the water environment.

MATERIALS AND METHODS

Study area

Hongqi mine is located at Xiangtan city (111°58′~113°05′ E, 27°21′~28°05′ N), Hunan Province, south central China, at an average altitude of 97.39 m. The mine covers 2.6 km^2 in a mountainous area. The climate type is subtropical monsoon and moist, with average temperatures of 16.7–17.4 °C; the maximum wind speed can be up to 17 m/s. Precipitation is abundant, and the annual precipitation is 1,200–1,500 mm, with between 60 and 80% falling between April and October (Fang *et al.* 2006; Jiang *et al.* 2018). In this study, the sampling points were distributed at intervals of 0.04–0.06 km^2 to make a total of 43 sampling points. These were divided into four regions: S1–S6 and S43 are Region 1, S7–S23 is Region 2, S24–S30 is Region 3, and S31–S42 is Region 4. The distribution of the sampling points is shown in Figure 1.

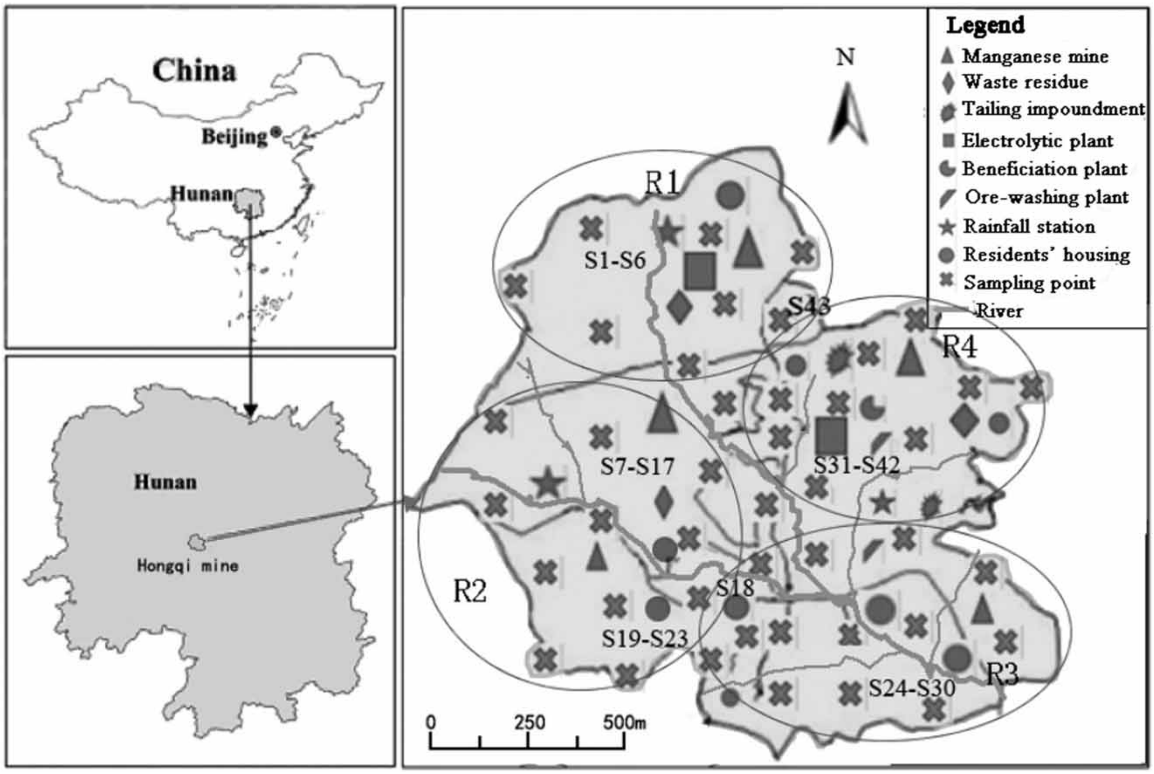

Figure 1 | Sampling location map.

Sample selection and analysis

In September–October 2018, 0.5–3 L rainwater runoff water samples were taken at each sample point and transferred to polypropylene containers. A total of five sub-samples were collected at each location based on a 5 m radius circle (points at east, west, south, north, and center) and mixed into a composite sample. The containers were packed in a black plastic bag with ice to ensure the freshness of the water samples. Subsequently, the water samples were shaken until homogeneous water samples were obtained, followed by a natural settlement time of 20–30 min, then the samples were siphoned and filtered through a 0.45 μm filter membrane. The filtrate was acidified to pH <2 using hydrochloric acid and nitric acid for future analysis (Ren *et al.* 2015).

The water samples were digested using the HCl-HNO_3 method (Ren *et al.* 2014). The concentrations of Mn, Cu and Zn were analyzed by flame atomic absorption spectrometry (AA7003A, Dongxi Research Institute of Electronics Technology, China). The detection limits (μg/L) for Mn, Cu and Zn were 0.1, 1 and 0.8 respectively. Other elements (Ni, Pb and Cd) were measured using graphite furnace atomic absorption spectrometry (Ren *et al.* 2015). The detection limits (μg/L) for Ni, Pb and Cd were 0.054, 0.05 and 0.012 respectively. In order to control the accuracy of the sample analyses, the standard reference material of the China National Standards Research Center: GBW (E) 080194 was used, and each sample was subjected to reagent blank and three repeated tests. The recovery rates of the target PTEs in the standard references were good and ranged between 94 and 106%.

In addition, a standard recovery experiment was performed to verify the precision of the test method (Ren *et al.* 2015). The recovery rates of Mn, Ni, Cu, Zn, Cd, and Pb were between 96.2% and 103.9%.

Health risk assessment

Health risk assessment is defined as the process of estimating the probability of occurrence of events and the possible magnitude of adverse health effects over a specified time period (Lim *et al.* 2008). For the assessment of the health risks of PTEs in the water environment, direct intake of rainwater as drinking water and skin absorption from rainwater on the human body are usually considered (Zeng *et al.* 2015). Locally relevant factors were used in the application of a standard risk assessment model (USEPA 2004), where the exposure doses for direct intake ($ADD_{ingestion}$) and skin absorption (ADD_{dermal}) were as follows (with ADD being the chronic daily intake of PTEs in μg/kg/day):

$$ADD_{ingestion} = \frac{C_w * IR * ABS_g * EF * ED}{BW * AT}$$

$$ADD_{dermal} = \frac{C_w * SA * K_p * EF * ET * ED}{BW * AT} \times 10^{-3}$$

where C_w is the concentration (μg/L). IR is the intake rate (L/day); 2.0 for adults and 0.64 for children in this study (Wang *et al.* 2017). ABS_g is a gastrointestinal absorption factor; in this study, they were 6.0%, 4.0%, 57%, 20%, 5.0% and 11.7% for Mn, Ni, Cu, Zn, Cd and Pb, respectively (Wang *et al.* 2017). EF is the exposure frequency (day/year), which was 350 in this study (Zeng *et al.* 2015). ED is the duration of exposure (year); 70 for adults and 6 for children in this study (USEPA 2004). BW is the residents' weight (kg), according to the survey of local residents; 65 for adults and 20 for children. AT is the non-carcinogenic mean time (day); 25,550 for adults and 2,190 for children in this study (USEPA 2004). SA is the exposed skin area (cm^2); 18,000 for adults and 6,600 for children in this study (Wang *et al.* 2017). K_p is the skin permeability coefficient (cm/h); Mn, Cu, Cd, and Pb were 0.001 (USEPA 2004; Zeng *et al.* 2015), Ni was 0.004 (Zeng *et al.* 2015), Zn was 0.0006 (USEPA 2004). ET is the exposure time (h/day); 0.58 for adults and 1.0 for children in this study (Wang *et al.* 2017).

Potential non-carcinogenic risks are assessed by hazard quotient (HQ) (USEPA 2004). HQ is defined as the health hazards due to two paths of exposure (ingestion and skin contact) in a lifetime. $HQ > 1$ indicates that there may be non-carcinogenic risk, and the risk increases with the increase in HQ value.

$$HQ = \frac{ADD}{RfD}$$

where RfD is the reference dose obtained from a risk-based centralized database (USEPA 2013). RfD_{dermal} and $RfD_{ingestion}$ are listed in Table 4.

The hazard index (HI) was used to assess the total potential non-carcinogenic risk caused by different pathways.

$$HI = \sum HQ_{ing} + HQ_{der}$$

As for HQ, when $HI > 1$, there may be non-carcinogenic risk, and the risk increases as the HQ value increases (USEPA 2004).

Carcinogenic risk (CR) is defined as the increasing probability that an individual will develop cancer in their lifetime due to chemical exposure in a given situation (Chen & Liao 2006). For this study, the carcinogenic risk of both Cd and Pb elements through both ingestion and skin absorption was calculated as follows:

$$CR = \sum ADD_i \times SF_i$$

where ADD_i is the daily intake by ingestion or skin absorption. SF_i (kg·day/mg) is the slope factor of carcinogens. The values are based on the USEPA risk concentration table: Cd is 6.3 and Pb is 8.5×10^{-3}. When $CR < 1 \times 10^{-6}$, the carcinogenic risk of rainwater runoff to health is negligible. When $CR > 1 \times 10^{-4}$, the carcinogenic risk in the local residents is high and unacceptable. When $1 \times 10^{-6} < CR < 1 \times 10^{-4}$, there is a certain chance of carcinogenic risk for local residents, but it is acceptable.

Statistical analysis

Descriptive statistics of water samples were performed using SPSS 22 (IBM, USA) software. The Pearson correlation coefficient matrix can be used to analyze correlations between various elements and provide effective information for explaining the sources of PTEs in the environment (Manta *et al.* 2002). ArcGIS 10.3 (ESRI, Redlands, California, USA) visually displays hot spots of PTEs in a study area. In addition, EPA PMF software (version 5.0) was used to analyze potential sources of PTEs in water samples. In PMF, non-negativity constraints can be imposed on factor elements and measurements can be weighted individually based on uncertainties when determining the least squares fit. With these features, PMF is a significant improvement over previous PCA techniques for receptor modeling of environmental data.

RESULTS AND DISCUSSION

Water contamination by PTEs

Table 1 lists descriptive statistics for the basic parameters of the samples and the concentrations of PTEs. The average concentration of PTEs (mg/L) were: 0.3357 (Mn), 0.0450 (Ni), 0.0106 (Cu), 0.0148 (Zn), 0.0068 (Cd) and 0.0390 (Pb), which agree very well with a previous site assessment (Ren *et al.* 2015). Except for Cu and Zn, the average concentration of the PTEs was higher than their corresponding standard values (Ministry of Health 2006). The maximum concentration (mg/L) of PTEs exceeding the standard value were: 3.0419 (Mn), 1.9331 (Ni), 0.2881 (Cd) and 1.6740 (Pb), by 30 times, 97 times, 58 times and 167 times the standard values, respectively. The sustained release of PTEs in mining activities leads to an increase in local concentrations and is enhanced by large amounts of organic matter in sediments and water (Neiva *et al.* 2016).

The coefficient of variation (CV) of PTEs are shown in Table 1. The CV values of Mn and Zn were 188.1% and 135.0%, respectively, showing very high variability. The CV values of Ni, Cu, Cd and Pb were 91.2%, 72.1%, 75.1% and 82.3%, respectively, showing high variability. High variability indicates the presence of discrete inputs related to natural or external factors. The high variability of PTEs suggests that they may be mainly derived from human inputs such as mining, industrial activities, and agricultural irrigation.

A comparison of PTEs in the rainwater runoff of Xiangtan manganese mine with those in rivers from other parts of China and internationally is presented in Table 2. The average concentration of PTEs was higher than the world average. Compared with other rivers in China, except for Mn, the average concentration of PTEs was lower than that of the Huaihe River (Wang *et al.* 2017), while higher than the Chinese Loess Plateau (CLP) rivers and the Pearl River (Geng *et al.* 2015; Xiao *et al.* 2019a). Compared with rivers in other countries, except for Mn and Pb, the average concentration of PTEs was lower than the Damodar River, India (Pal & Maiti 2018), while higher than in Catalan rivers, Spain (Carafa *et al.* 2011). The levels observed show a moderate order of magnitude of PTE pollution in the rainwater runoff area.

The most suitable interpolation applied to one heavy metal could be selected by comparing average error and root mean square error, which was generated from Kriging, inverse distance weighted (IDW) and radial basis function (RBF) by comparing the average error, the response error range and the root mean square error response sensitivity. By comparing the three interpolation methods, the results showed that the RBF method was the best for Mn, Ni, Cu and Cd, Kriging interpolation for Zn and Pd.

Table 1 | Statistical analysis of PTE concentrations (mg/L) and basic parameters in water samples

Element	Mn	Ni	Cu	Zn	Cd	Pb
Minimum	0.0049	0.023	0.0014	0.0014	0.0001	0.007
Maximum	3.0419	1.9331	0.4516	0.6385	0.2881	1.674
Mean	0.3357	0.0450	0.0106	0.0148	0.0068	0.0390
Median	0.0511	0.0325	0.0089	0.0095	0.0067	0.0300
Standard deviation	0.6341	0.0414	0.0077	0.0204	0.0053	0.0322
CV (%)	188.1	91.2	72.1	135.0	75.1	82.3
Skewness	2.716	1.725	1.365	3.459	2.094	1.275
Kurtosis	8.117	3.213	1.772	13.426	6.891	1.013
Standard values	0.1	0.02	1	1	0.005	0.01

Table 2 | Comparison of PTE concentrations (mg/L) in rainwater runoff from Xiangtan manganese mine with other rivers in the world

Rivers	Mn	Ni	Cu	Zn	Cd	Pb	References
Rainwater runoff from Xiangtan manganese mine	0.3357	0.0450	0.0106	0.0148	0.0068	0.0390	This study
Huaihe River	0.0490	0.0462	0.0523	10.504	0.0617	0.1550	Wang *et al.* (2017)
Pearl River	0.0011	0.0019	0.0011	0.0036	0.04×10^{-3}	0.0008	Geng *et al.* (2015)
Rivers in CLP	0.0712	0.0054	0.0051	0.0066	0.03×10^{-3}	0.0003	Xiao *et al.* (2019a)
Damodar River, India	0.033	0.052	0.018	0.089	0.009	0.0100	Pal & Maiti (2018)
Catalan rivers, spain		0.0027	0.0013	0.0019	0.0012	0.0022	Carafa *et al.* (2011)
World average	0.034	0.0008	0.0015	0.0006	0.08×10^{-3}	0.08×10^{-3}	Gaillardet *et al.* (2014)

The hot spot areas and potential sources of contamination can be identified by a hot spot map of PTE concentrations (Li *et al.* 2017). The most appropriate interpolation was performed on all samples as a digital mapping method to obtain visual information on the contamination of PTEs. The results are shown in Figure 2. There were obvious differences in the pollution and content of PTEs: the contaminated area of Mn, Cu, Zn and Pb were similar, mainly distributed in the northeast of the study area and related to industrial activities, especially direct mining, smelting, and tailings. Ni was mainly distributed in the south of the study area, where the majority of the regional population lives. The pollution from Cd was more dispersed, which may be related to intensive agricultural production and residential areas having aggregated inputs from multiple sources.

Source analysis of PTEs

The Pearson correlation analysis is an effective way to explore the relationship between multiple data as an initial

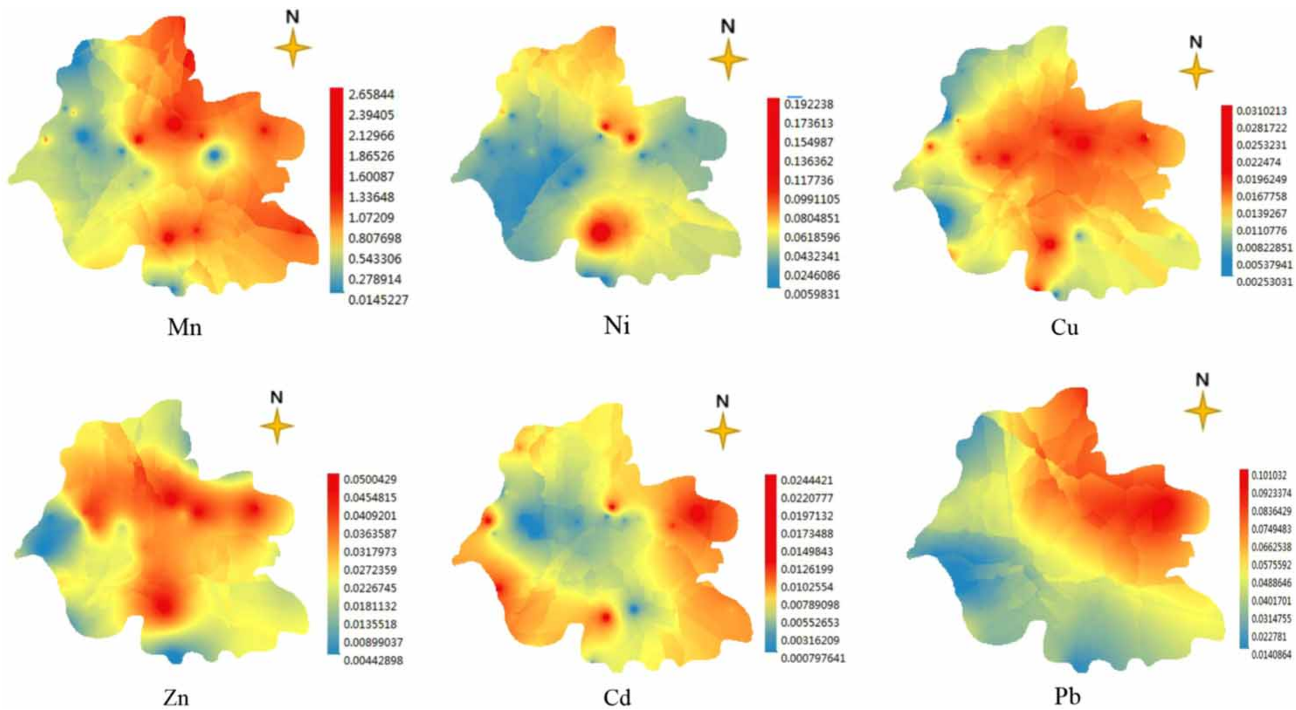

Figure 2 | Spatial distribution of each PTE (mg/L).

screening approach (Al-Khashman & Shawabkeh 2006). The Pearson correlation coefficient calculation results are shown in Table 3. In this study, Mn and Ni showed a moderate correlation ($r^2 = 0.576$**) and Zn and Pb showed a moderate correlation ($r^2 = 0.605$**) at a significance level of 0.01. In addition, Cu and Zn ($r^2 = 0.609$**), Zn and Cd ($r^2 = 0.578$**), and Cu and Pb ($r^2 = 0.113$**) were all moderately correlated. Strong correlations between metals indicate their potential common source and similar diffusion pathways (Forghani *et al.* 2015), and may be related to their chemical nature (Sungmin *et al.* 2012). Zn and Ni ($r^2 = 0.436$**), Zn and Pb ($r^2 = 0.434$**), Pb and Cd ($r^2 = 0.456$**), Mn and Cu ($r^2 = 0.342$**) and Mn and Cd ($r^2 = 0.499$**) all showed low correlations.

Table 3 | Correlation coefficients between heavy metal concentrations from site samples

	Mn	Ni	Cu	Zn	Cd	Pb
Mn	1					
Ni	0.576**	1				
Cu	0.342*	0.119	1			
Zn	0.578**	0.436**	0.609**	1		
Cd	0.499**	0.307*	0.250	0.578**	1	
Pb	0.605**	0.251	0.513**	0.434**	0.456**	1

** indicates that the correlation reached a significance level of 0.01 (two-tailed).
* indicates that the correlation reached a significance level of 0.05 (two-tailed).

Based on the analysis of the PMF model, four factors were identified for possible sources of PTEs in rainwater runoff. Figure 3 shows the result of PMF with the factor contributions for each element and the derived source fingerprint. The PMF input data includes concentration data (six elements for 43 samples) and their corresponding uncertainty data. In order to ensure the rationality of the model, Mn, Ni, Cu, Zn, Cd and Pb were set as strong, strong, strong, strong, weak and strong, respectively, according to the signal-to-noise ratio (S/N). The number of factors run was set as 3, 4, and 5, the start seed number was chosen randomly and the number of runs was set as 20. When the number of source factors is set to 5, the Q value is the most stable and minimal. Further, the model fitting (R^2) was 0.998, 0.886, 0.986, 0.999, and 0.863 for Mn, Ni, Cu, Zn, and Pb, respectively. The R^2 values being above 0.7 indicates that the model is appropriate and the data is reliable (Huang *et al.* 2018). The results provide much greater detail of factor separation compared to the limited resolution from PCA analysis in the study by Ren *et al.* (2015).

The first factor is dominated by Cu and Pb, with contributions of 72.6% and 28.4%, respectively. According to field investigations, we found higher levels of Cu and Pb in the

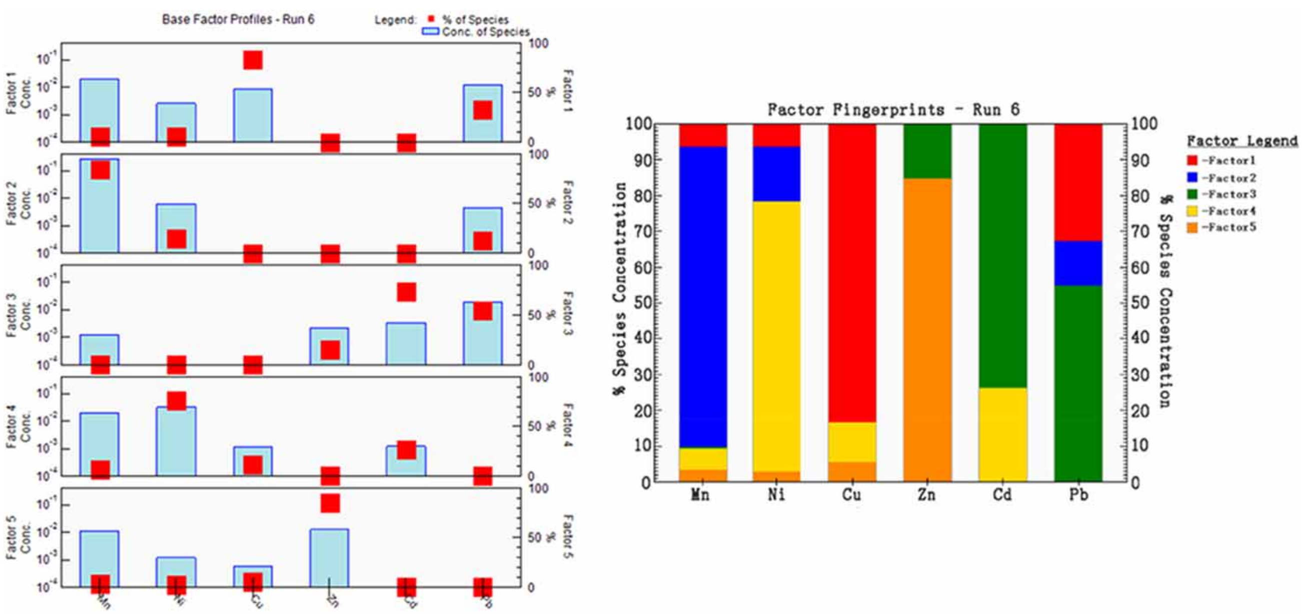

Figure 3 | Factor distribution and source contribution of PTEs in the PMF model.

samples located around the smelter and on both sides of the road. Therefore, the high concentrations of Cu may be derived directly from manganese mining activities, especially smelting. In addition, the wear on tires and brake linings is the main source of Cu in runoff, with a lower contribution from Pb due from the combustion of leaded gasoline (Zhang *et al.* 2016). Although China has banned the use of leaded gasoline since 2000, there have been some recent reports of elevated Pb content in roadside runoff (Chen *et al.* 2018). Therefore, factor 1 can be considered to be derived from smelting and traffic emissions.

The second factor is dominated by Mn, with a contribution of 87.3% associated with a small contribution from Ni and Pb. According to field investigations, high concentrations of Mn may be directly derived from manganese ore activities, such as mining and tailings. The association of Ni with Mn may also be derived from the ore as associated elements. The main source of Pb is traffic emissions, which may be related to ore transportation in the mining area. Therefore, the factor 2 can be considered to be derived from mining activities.

The third factor is related to Cd and Pb, and the contribution were 73.7% and 54.7%, respectively. Cd may be derived from some municipal sewage, pesticides and fertilizers, and atmospheric deposition (Rehman *et al.* 2018). As an additive, Cd has been widely used as a pesticide and has been associated with phosphate fertilizer in agricultural production in China. However, many scientists insist that atmospheric deposition is the source of Cd accumulation, not the use of pesticides and fertilizers (Yi *et al.* 2018). According to a study in Hunan Province (Yi *et al.* 2018), atmospheric deposition was found to be the main source of Cd and Zn in soil, with a contribution of over 90%. However, there was not a large accumulation of Zn in factor 3 in this study. The main sources of Pb are historic traffic emissions in addition to primary ore activities. Pb may also be related to the transportation of agricultural products in factor 3.

The fourth factor is dominated by Ni and Cd, with contributions of 75.7% and 26.3%, respectively. Some studies report that Ni is mainly derived from natural sources and industrial emissions (Chen *et al.* 2016). High concentrations of Ni may be associated with electronics and electroplating industry products such as electronic waste, electroplating pipes, etc (Skowroński *et al.* 2015). However, the average concentration of Ni was almost equal to the standard value in this study, indicating that the Ni concentration was mostly within the allowable range. Cd also accounts for a certain proportion of factor 4; additional Cd may be derived from some municipal sewage, pesticides and fertilizers, and atmospheric deposition (Rehman *et al.* 2018). However, factor 4 is mainly Ni, and the source of Cd is only secondary. Therefore, factor 4 can be considered to be derived from natural sources.

Factor 5 is mainly Zn, with a contribution of 81.1%. A large amount of Zn is also associated with direct manganese ore activities, especially smelting activities (Liang *et al.* 2016). The element has a relatively low melting point and vapor generated during ore smelting and pollution control enriches this element in wastes, with potential for wastewater discharge. A number of studies have shown the accumulation of Zn around smelters due to dry/wet precipitation of metal-containing particles (Ran *et al.* 2017). Therefore, factor 5 can be considered to be derived from smelting activities.

Health risk assessment of PTEs

Using the health risk assessment method to evaluate the elements in the rainwater runoff in the manganese mining area of Xiangtan city, the non-carcinogenic risks to adults and children under different exposure conditions (Table 4, Figure 4) and carcinogenic risks (Table 5, Figure 4) were obtained. The results show that the mean values of $HQ_{ingestion}$, HQ_{dermal}, and HI were both <1 (Table 4), indicating that these elements do not pose a non-carcinogenic risk to local people in this study through surface water contamination. The total HI for adults was 0.292, of which Pb accounted for 37.74%, Mn accounted for 26.93%, and Cd accounted for 20.90%. For children, the total HI value was 0.45, of which Mn accounts for 30.32%, Pb accounts for 28.69%, and Cd accounts for 23.41%. Therefore, Mn, Cd and Pb were the main elements of non-carcinogenic risk. Adults and children had similar health risks from ingestion, but the health risks from skin absorption were twice the size for children than for adults (Table 4). The predicted ingestion of PTEs by

Table 4 | Reference dose (RfD), risk quotient (HQ), and risk index (HI) values of individual elements in the Xiangtan manganese mining area

			$HQ_{ingestion}$		HQ_{dermal}		$HI = \sum HQs$	
Element	$RfD_{ingestion}$ (μg/kg/day)	RfD_{dermal} (μg/kg/day)	Adult	Child	Adult	Child	Adult	Child
Mn	24	0.96	2.48×10^{-2}	2.58×10^{-2}	5.39×10^{-2}	1.11×10^{-1}	7.87×10^{-2}	1.36×10^{-1}
Ni	20	0.8	2.65×10^{-3}	2.76×10^{-3}	3.46×10^{-2}	7.11×10^{-2}	3.73×10^{-2}	7.39×10^{-2}
Cu	40	12	4.42×10^{-3}	4.59×10^{-3}	1.35×10^{-4}	2.77×10^{-4}	4.55×10^{-3}	4.87×10^{-3}
Zn	300	60	2.92×10^{-4}	3.04×10^{-4}	2.29×10^{-5}	4.70×10^{-5}	3.15×10^{-4}	3.51×10^{-4}
Cd	0.5	0.025	1.98×10^{-2}	2.06×10^{-2}	4.13×10^{-2}	8.48×10^{-2}	6.10×10^{-2}	1.05×10^{-1}
Pb	1.4	0.42	9.60×10^{-2}	9.98×10^{-2}	1.43×10^{-2}	2.93×10^{-2}	1.10×10^{-1}	1.29×10^{-1}
Total			1.48×10^{-1}	1.54×10^{-1}	1.44×10^{-1}	2.96×10^{-1}	2.92×10^{-1}	4.50×10^{-1}

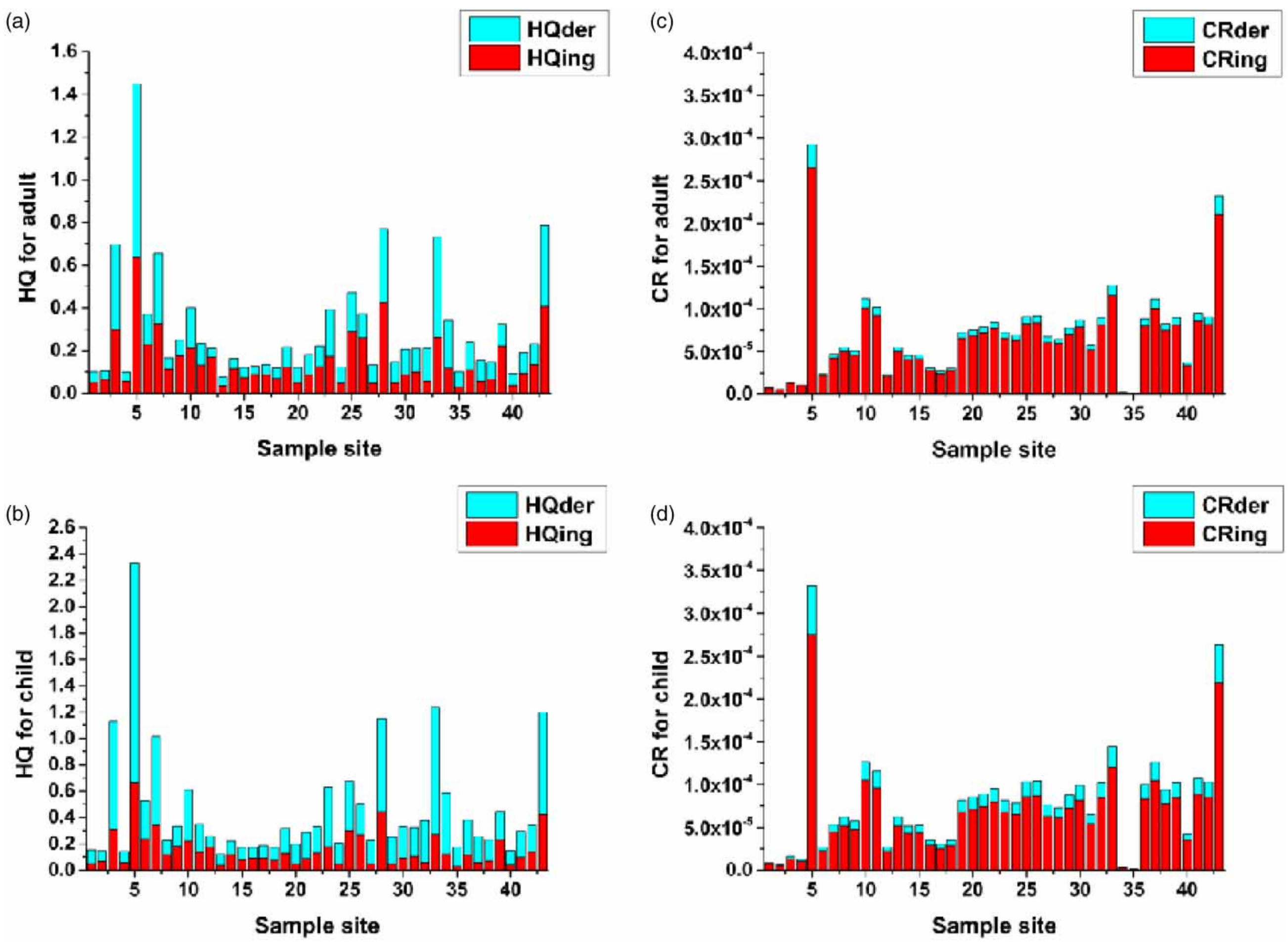

Figure 4 | Non-carcinogenic risk of PTEs in the sample point rainwater runoff: (a) (adult) and (b) (children). Sample point rainwater runoff PTE carcinogenic risk: (c) (adult) and (d) (children).

adults and children accounted for 50.6% and 34.2%, respectively, of the non-carcinogenic risk. Skin absorption accounted for 49.4% and 65.8%, respectively.

The carcinogenic risk of the elements Cd and Pb was calculated (Table 5). For adults and children, the average carcinogenic risk of rainwater runoff was 7.00×10^{-5} and

Table 5 | Carcinogenic risk in adults and children by different pathways

Element	Cd	Cd	Pb	Pb	Total
Pathway	CR_{ing}	CR_{der}	CR_{ing}	CR_{der}	TCR
Adult	6.23×10^{-5}	6.50×10^{-6}	1.14×10^{-6}	5.09×10^{-8}	7.00×10^{-5}
Child	6.48×10^{-5}	1.34×10^{-5}	1.19×10^{-6}	1.05×10^{-7}	7.94×10^{-5}

7.94×10^{-5}, respectively. This indicates that children were more vulnerable than adults to carcinogenic risk. The carcinogenic risk value was lower than 1.00×10^{-4} for both adults and children, but both were higher than 1.00×10^{-6}, which indicates that local adults and children may be affected by increased carcinogenic risk, but at an acceptable level. The carcinogenesis risk by ingestion was significantly higher than by skin absorption (Table 5, Figure 4), and ingestion of Cd was a major contributor. For adults and children, it accounted for 89% and 81.55%, respectively, of the total carcinogenic risk, respectively, while skin absorption of Cd accounted for 9.3% and 16.9%, respectively. In this study, although the carcinogenic risk generated was not severe, it is prudent to carry out monitoring in the study area, especially for Cd.

CONCLUSION

This study evaluated the pollution, source and health risks of PTEs in the rainwater runoff in the Xiangtan mining area. The average concentrations of Mn, Ni, Cd and Pb exceed their standard values. The CV values of Mn and Zn show very high variability, indicating that they are greatly influenced by industrial activities. Compared to other locations (and other media – such as soils), the level of pollution in runoff waters in the Xiangtan mining area is at a medium level. The results of the interpolation processes in the GIS show that the contaminated areas of Mn, Cu, Zn and Pb are similar, mainly distributed in the northeastern region where industrial activities are most concentrated. For Ni, distribution is focused in the southern part of the site close to the majority of the residential population, while Cd is more dispersed. Source identification of PTEs helps identify areas of priority control, and assessment of health risks is important to determine the relative contribution of specific elements in a particular area to health hazards. The source analysis results based on the PMF model produced a higher resolution of contributions than the previously applied PCA approach and extracted four different sources of PTE from the wider environment. For Mn, inputs were mainly derived from mining activities, and additional contributions of Cu, Cd and Pb came from traffic emissions and agricultural activities in the area. A clear dominant input for Zn is likely to be from smelting activities. The health risk assessment showed that the non-carcinogenic risk in this study was low and negligible. Carcinogenic risks, however, were more significant for both adults and children, with children being more vulnerable, especially to the potential ingestion of Cd.

The use of PMF has improved source apportionment that fits with industrial activities in the area and spatial assessment focuses on priority areas for surface water management. The results of this study will provide effective information for further prevention of PTE pollution and provide a scientific basis for health risk assessment in water environments.

ACKNOWLEDGEMENTS

This work was supported by the National Natural Science Foundation of China (No. 41973078) and the Ministry of Education in China Project of Humanities and Social Science (2019JJ40081).

DATA AVAILABILITY STATEMENT

All relevant data are included in the paper or its Supplementary Information.

REFERENCES

Al-Khashman, O. A. & Shawabkeh, R. A. 2006 Metals distribution in soils around the cement factory in southern Jordan. *Environmental Pollution* **140** (3), 387–394.

Bellanco, M. J. & Sánchez-Leal, R. F. 2016 Spatial distribution and intra-annual variability of water masses on the Eastern Gulf of Cádiz seabed. *Continental Shelf Research* **128**, 26–35.

Cao, X., Diao, M., Zhang, B., Liu, H., Wang, S. & Yang, M. 2017 Spatial distribution of vanadium and microbial community responses in surface soil of Panzhihua mining and smelting area, China. *Chemosphere* **183**, 9–17.

Carafa, R., Faggiano, L., Real, M., Munne, A., Ginebreda, A., Guasch, H., Flo, M., Tirapu, L. & von der Ohe, P. C. 2011 Water toxicity assessment and spatial pollution patterns identification in a Mediterranean River Basin District. Tools for water management and risk analysis. *Science of the Total Environment* **409** (20), 4269–4279.

Chen, H., Chen, R., Teng, Y. & Wu, J. 2016 Contamination characteristics, ecological risk and source identification of trace metals in sediments of the Le'an River (China). *Ecotoxicology and Environment Safety* **125**, 85–92.

Chen, S. C. & Liao, C. M. 2006 Health risk assessment on human exposed to environmental polycyclic aromatic hydrocarbons pollution sources. *Science of the Total Environment* **366** (1), 112–123.

Chen, L., Zhou, S., Shi, Y., Wang, C., Li, B., Li, Y. & Wu, S. 2018 Heavy metals in food crops, soil, and water in the Lihe River Watershed of the Taihu Region and their potential health risks when ingested. *Science of the Total Environment* **615**, 141–149.

Fang, X., Tian, D. L. & Xie, R. X. 2006 Soil physical and chemical properties of the wasteland in Xiangtan manganese mine. *Acta Ecologica Sinica* **26** (5), 1494–1501.

Forghani, G., Mokhtari, A. R., Kazemi, G. A. & Fard, M. D. 2015 Total concentration, speciation and mobility of potentially toxic elements in soils around a mining area in central Iran. *Chemie der Erde – Geochemistry – Interdisciplinary Journal for Chemical Problems of the Geosciences and Geoecology* **75** (3), 323–334.

Gaillardet, J., Viers, J. & Dupré, B. 2014 Trace Elements in River Waters. In: *Treatise on Geochemistry (Second Edition)*, Holland, H. D. & Turekian, K. K. (eds), Elsevier, Oxford, volume 7, pp. 195–235.

Geng, J., Wang, Y. & Luo, H. 2015 Distribution, sources, and fluxes of heavy metals in the Pearl River Delta, South China. *Marine Pollution Bulletin* **101** (2), 914–921.

Herbert Jr., R. B., Winbjörk, H., Hellman, M. & Hallin, S. 2014 Nitrogen removal and spatial distribution of denitrifier and anammox communities in a bioreactor for mine drainage treatment. *Water Research* **66** (66), 350–360.

Huang, J., Guo, S., Zeng, G. M., Li, F., Gu, Y., Shi, Y., Shi, L., Liu, W. & Peng, S. 2018 A new exploration of health risk assessment quantification from sources of soil heavy metals under different land use. *Environmental Pollution* **243** (Pt A), 49–58.

Huang, J., Shi, Y., Zeng, G., Gu, Y., Chen, G., Shi, L., Hu, Y., Tang, B. & Zhou, J. 2016 Acyl-homoserine lactone-based quorum sensing and quorum quenching hold promise to determine the performance of biological wastewater treatments: an overview. *Chemosphere* **157**, 137–151.

Jiang, F., Ren, B., Hursthouse, A. S. & Zhou, Y. 2018 Trace metal pollution in topsoil surrounding the Xiangtan Manganese Mine Area (South-Central China): source identification, spatial distribution and assessment of potential ecological risks. *International Journal of Environmental Research and Public Health* **15** (11), 2412.

Li, K., Gu, Y., Li, M., Lin, Z., Ding, J., Lun, Z. & Wen, T. 2017 Spatial analysis, source identification and risk assessment of heavy metals in a coal mining area in Henan, Central China. *International Biodeterioration & Biodegradation* **128**, S0964830517304766.

Li, Y., Yang, X., Bing, G. & Xue, L. 2018 Effective bioremediation of Cu(II) contaminated waters with immobilized sulfate-reducing bacteria-microalgae beads in a continuous treatment system and mechanism analysis. *Journal of Chemical Technology & Biotechnology* **93** (5), 1453–1461.

Liang, J., Liu, J., Yuan, X., Zeng, G., Yuan, Y., Wu, H. & Li, F. 2016 A method for heavy metal exposure risk assessment to migratory herbivorous birds and identification of priority pollutants/areas in wetlands. *Environmental Science and Pollution Research International* **23** (12), 11806–11813.

Lim, H. S., Lee, J. S., Chon, H. T. & Sager, M. 2008 Heavy metal contamination and health risk assessment in the vicinity of the abandoned Songcheon Au–Ag mine in Korea. *Journal of Geochemical Exploration* **96** (2), 223–230.

Liu, J., Cao, L. & Dou, S. 2017 Bioaccumulation of heavy metals and health risk assessment in three benthic bivalves along the coast of Laizhou Bay, China. *Marine Pollution Bulletin* **117** (1–2), 98–110.

Manta, D. S., Angelone, M., Bellanca, A., Neri, R. & Sprovieri, M. 2002 Heavy metals in urban soils: a case study from the city of Palermo (Sicily), Italy. *Science of the Total Environment* **300** (1–3), 229–243.

Ministry of Health P 2006 In: *GB5749–2006, Standards for Drinking Water Quality*. Ministry Of Health, PRC, Beijing.

Neiva, A. M. R., Cunha, P. P. & Costa, M. M. 2016 Spatial variability of soils and stream sediments and the remediation effects in a Portuguese uranium mine area. *Chemie der Erde – Geochemistry – Interdisciplinary Journal for Chemical Problems of the Geosciences and Geoecology* **76** (4), S000928191630143X.

Pal, D. & Maiti, S. K. 2018 Heavy metal speciation, leaching and toxicity status of a tropical rain-fed river Damodar, India. *Environ Geochem Health* **40** (6), 2303–2324.

Pareja-Carrera, J., Mateo, R. & Rodriguez-Estival, J. 2014 Lead (Pb) in sheep exposed to mining pollution: implications for animal and human health. *Ecotoxicology and Environment Safety* **108** (108C), 210–216.

Ran, X., Shuang, W., Li, R., Wang, J. J. & Zhang, Z. 2017 Soil heavy metal contamination and health risks associated with artisanal gold mining in Tongguan, Shaanxi, China. *Ecotoxicology & Environmental Safety* **141**, 17–24.

Rehman, M. Z. U., Rizwan, M., Hussain, A., Saqib, M., Ali, S., Sohail, M. I., Shafiq, M. & Hafeez, F. 2018 Alleviation of cadmium (Cd) toxicity and minimizing its uptake in wheat (Triticum aestivum) by using organic carbon sources in Cd-spiked soil. *Environmental Pollution* **241**, 557–565.

Ren, B., Hongpu, M. A., Zheng, X., Liu, B. & Zhou, Y. 2014 Spatial structure characteristics of heavy metal content and pollution levels of rainfall runoff in manganese ore zone. *Acta Scientiae Circumstantiae* **34** (7), 1730–1737.

Ren, B., Wang, Q., Chen, Y., Ding, W. & Zheng, X. 2015 Analysis of the metals in soil-water interface in a manganese mine. *Journal of Analytical Methods in Chemistry* **2015** (1), 163163.

Ren, B., Zhou, Y., Hursthouse, A. S. & Deng, R. 2017 Research on the characteristics and mechanism of the cumulative release of antimony from an antimony smelting slag stacking area under rainfall leaching. *Journal of Analytical Methods in Chemistry* **2017** (4), 7206876.

Skowroński, J. M., Rozmanowski, T. & Osińska, M. 2015 Reuse of nickel recovered from spent Ni–Cd batteries for the preparation of C/Ni and C/Ni/Pd layered electrodes for energy sources. *Process Safety & Environmental Protection* **93**, 139–146.

Soonthornnonda, P. & Christensen, E. R. 2008 Source apportionment of pollutants and flows of combined sewer wastewater. *Water Research* **42** (8–9), 1989–1998.

Sungmin, H., Tseren-Ochir, S. E., Hee Jin, H., Bum, H. S., Soon Do, H. & Hidaeki, M. 2012 Evidence of global-scale As, Mo, Sb, and Tl atmospheric pollution in the antarctic snow. *Environmental Science & Technology* **46** (21), 11550–7.

Tang, Z., Chai, M., Cheng, J., Jin, J., Yang, Y., Nie, Z., Huang, Q. & Li, Y. 2017 Contamination and health risks of heavy metals in street dust from a coal-mining city in eastern China. *Ecotoxicology and Environment Safety* **138**, 83–91.

USEPA 2004 Risk Assessment Guidance for Superfund Volume I: Human Health Evaluation Manual (Part E, Supplemental Guidance for Dermal Risk Assessment). In: *EPA/540/R/99/005*. Office of Superfund Remediation and Technology Innovation U.S., Environmental Protection Agency, Washington, DC.

USEPA 2013 *Risk-based Concentration Table*. Available from: http://www.epa.gov/region9/superfund/prg/.

Wang, J., Liu, G., Liu, H. & Lam, P. K. S. 2017 Multivariate statistical evaluation of dissolved trace elements and a water quality assessment in the middle reaches of Huaihe River, Anhui, China. *Science of the Total Environment* **583**, 421–431.

Xiao, J., Wang, L., Deng, L. & Jin, Z. 2019a Characteristics, sources, water quality and health risk assessment of trace elements in river water and well water in the Chinese Loess Plateau. *Science of the Total Environment* **650** (Pt 2), 2004–2012.

Xiao, R., Guo, D., Ali, A., Mi, S., Liu, T., Ren, C., Li, R. & Zhang, Z. 2019b Accumulation, ecological-health risks assessment, and source apportionment of heavy metals in paddy soils: a case study in Hanzhong, Shaanxi, China. *Environmental Pollution* **248**, 349–357.

Yang, Z., Wu, Z., Liao, Y., Liao, Q., Yang, W. & Chai, L. 2017 Combination of microbial oxidation and biogenic schwertmannite immobilization: a potential remediation for highly arsenic-contaminated soil. *Chemosphere* **181**, 1–8.

Yang, Z., Liang, L., Yang, W., Shi, W., Tong, Y., Chai, L., Gao, S. & Liao, Q. 2018 Simultaneous immobilization of cadmium and lead in contaminated soils by hybrid bio-nanocomposites of fungal hyphae and nano-hydroxyapatites. *Environmental Science and Pollution Research International* **25** (12), 11970–11980.

Yang, Q. W., Xu, Y., Liu, S. J., He, J. F. & Long, F. Y. 2011 Concentration and potential health risk of heavy metals in market vegetables in Chongqing, China. *Ecotoxicology and Environment Safety* **74** (6), 1664–1669.

Yi, K., Fan, W., Chen, J., Jiang, S., Huang, S., Peng, L., Zeng, Q. & Luo, S. 2018 Annual input and output fluxes of heavy metals to paddy fields in four types of contaminated areas in Hunan Province, China. *Science of the Total Environment* **634**, 67–76.

Zeng, X., Liu, Y., You, S., Zeng, G., Tan, X., Hu, X., Hu, X., Huang, L. & Li, F. 2015 Spatial distribution, health risk assessment and statistical source identification of the trace elements in surface water from the Xiangjiang River, China. *Environmental Science and Pollution Research International* **22** (12), 9400–9412.

Zhang, Z., Wang, J. J., Ali, A. & DeLaune, R. D. 2016 Heavy metals and metalloid contamination in Louisiana Lake Pontchartrain Estuary along I-10 Bridge. *Transportation Research Part D: Transport and Environment* **44**, 66–77.

First received 15 May 2020; accepted in revised form 17 November 2020. Available online 16 December 2020